Research Square

Preprints are preliminary reports that have not undergone peer review.
They should not be considered conclusive, used to inform clinical practice,
or referenced by the media as validated information.

One-pot synthesis and in silico ADME profiling of 1,4-dihydropyridine derivatives catalyzed by ProMSA ionic liquid under solvent-free conditions

Nitin Rode

nrrode@nowrosjeewadiacollege.edu.in

Nowrosjee Wadia College

Kishor Kale

Nowrosjee Wadia College

Santosh Terdale

Savitribai Phule Pune University

Research Article

Keywords: Amino acid ionic liquid, dihydropyridine, ADME study, pharmacokinetic study

Posted Date: March 10th, 2026

DOI: https://doi.org/10.21203/rs.3.rs-8939554/v1

License: This work is licensed under a Creative Commons Attribution 4.0 International License.
Read Full License

Additional Declarations: No competing interests reported.

Abstract

An efficient and convenient method has been developed for the one-pot, four-component synthesis of 1,4-dihydropyridine derivatives. The protocol involves the reaction of aromatic aldehydes, β-keto esters, and ammonium acetate catalyzed by ProMSA, a Brønsted acidic amino acid ionic liquid (AAIL), under solvent-free conditions. This methodology offers several advantages, including the use of an inexpensive, easily prepared, and recyclable catalyst; a simple experimental procedure; and a green and safer reaction profile. The desired products were obtained in excellent yields with high purity following a straightforward workup and within short reaction times. Furthermore, *in silico* ADME study of all synthesized compounds was conducted. The results indicate that all derivatives obey Lipinski's rule of five, as well as the Ghose filter, Egan, and Muegge rules, suggesting favorable physicochemical properties, good oral bioavailability potential, and suitability for advanced pharmacokinetic investigations.

Introduction

The six-membered heterocyclic ring system containing a nitrogen atom at the 1-position, which is saturated at the 1 and 4 positions, is known as 1,4-dihydropyridine (1,4-DHP). This scaffold was first synthesized by Arthur Hantzsch in 1881 via a pioneering multicomponent reaction (MCR) [1]. The classical Hantzsch synthesis involves the one-pot condensation of a β-keto ester (a 1,3-dicarbonyl compound), an aromatic aldehyde, and ammonia or an ammonium salt to afford 1,4-dihydropyridine derivatives, commonly referred to as Hantzsch esters [2]. The stability of these compounds is significantly enhanced when the 3 and 5 positions are substituted with electron-withdrawing groups such as cyano (CN), carbonyl (COR), or ester (COOR) functionalities [3]. Nitrogen-containing heterocycles, particularly the 1,4-DHP scaffold, are frequently found in biologically and medicinally active compounds [4–6]. They are widely recognized for their therapeutic applications, most notably as calcium channel blockers (e.g., nifedipine, amlodipine, felodipine, Fig. 1). Additionally, they exhibit a broad spectrum of pharmacological activities, including anticonvulsant, antitumor, analgesic, and anti-inflammatory effects, and are extensively used in the treatment of cardiovascular diseases [7–11].

To improve the productivity of 1, 4-dihydropyridines synthesis, different catalyst have been used such as HY-Zeolite [13], ceric ammonium nitrate [14], Montmorillonite K10 [15], FeF_3 [16], Triton X-100 in water [17], HPW/PEG-400 [18], N-(phenylsulfonyl)benzene sulfonamide [19], Acid catalyst such as alumina sulfuric acid (ASA) [11], organocatalyst-succinic acid [20], polyphosphoric acid (PPA)@NiO [21], borotungstic acid $H_5BW_{12}O_{40}$ [22], Polyvinylpolypyrrolidone supported chlorosulfonic acid [23], Phosphinic Acid on UiO-66-NH_2 [24], Ionic liquid catalyst likes tetrabutylammonium hydrogen sulfate (TBAHS) [25], Tetrabutylphosphonium Dichromate (TBPDC) (MW) [26], mild acidic ionic liquids such as N-methyl-2-pyrrolidoniumdihydrogen phosphate [NMP][H_2PO_4] [27], ionic liquid sulfonic acid functionalized pyridinium chloride [28], Nanoparticle catalyst such as graphene oxide nano particles [29], nano-crystalline solid acid catalyst (nano-sulfated zirconia, nano-structured ZnO, nano-g-alumina and nano-ZSM-5 zeolites) [30], manganese ferrite nanoparticles ($MnFe_2O_4$) [31], Cu immobilized on $MgZnFe_2O_4$ nanoparticles [32], nano-Fe_3O_4@dextrin/BF_3 [33], nano-sized Magnesia–Zirconia (nano-MgO–ZrO_2)

catalyst [34], Fe_3O_4 hybrid nanocatalyst [35], Copper(I) Iodide Nanoparticles [36], Magnetic nanoparticles likes hercynite@sulfuric acid nanomagnetic solid acid catalyst [37], {$Fe_3O4@SiO_2@(CH2)_3Im$}$C(NO_2)_3$ magnetic nano particles [38], GO/Fe_3O_4/ZIF-67 magnetic nanocatalyst [39], Silica-Coated Magnetic $NiFe_2O_4$ Nanoparticles [40], Magnetic $MnFe_2O_4$ Nanoparticles [41], Magnetic Fe-C-O-Mo alloy nano-rods [42], $MgFe_2O_4$ MNPs [43], Metal catalyst like Fe_3O_4@chitosan [44], $AlCl_3.6H_2O$ [45], bismuth (III) chloride [46], PdRuNi@GO Catalyst [47], Aluminized polyborate-catalysed [48], Mn(II) on Fe_3O_4@ Schiff base [49], MCM-41 supported cobalt (II) complex [50], $TiCl_2$/Nano-γ-Al_2O_3 [51], Mn-MOFs [52], Neat, ultrasound and microware assisted synthesis includes catalyst like visible light promoted Praseodymium Oxide (Pr_6O_{11}) Seal Vessel [53], neat under solvent-free [54], ammonium bicarbonate (MW) [55], microwave assisted *o*-Iodoxybenzoic acid (IBX) [56], praseodymium oxide using visible light [57], Iodobenzene diacetate (III) by coventional heating, Ultrasound and MW [58], Ultrasound-assisted [59]. Some of the above methods for the synthesis of 1,4-dihydropyridines derivatives have one or more adverse points such as moisture sensitive, expensive reagents, tedious workup processes and harsh reaction conditions; thus, developing a proficient procedure with a potent catalyst for the synthesis of 1,4-dihydropyridine is still key importance. The physicochemical and pharmacokinetic properties of compounds were utilized to recognize the drug-likeness of compounds as a potential therapeutic drug candidate in an *in silico* ADME (absorption, distribution, metabolism, and excretion) study.

Experimental

General procedure for synthesis of 1, 4-dihydropyridine derivatives (5a-5g)

A round-bottom flask was charged with aromatic aldehyde (10 mmol), ethyl or methyl acetoacetate (20 mmol), ammonium acetate (15 mmol), and the AAIL catalyst ProMSA (10 mol%). The reaction mixture was stirred at 100˚C for the appropriate time, and progress was monitored by TLC. Upon completion, the reaction mixture was cooled to room temperature, and ethanol (10 mL) was added. The mixture was stirred for 30 minutes to obtain the crude solid product. The solid was collected by filtration using Whatman filter paper, washed thoroughly with cold ethanol and hexane to remove traces of aldehyde, and recrystallized from ethanol if necessary.

General procedure for synthesis of 1, 4-dihydropyridine derivatives (6a-6g)

A round-bottom flask was charged with dimedone (10 mmol), aromatic aldehyde (10 mmol), ethyl or methyl acetoacetate (10 mmol), ammonium acetate (15 mmol), and the AAIL catalyst ProMSA (10 mol%). The reaction mixture was stirred at 100˚C for the appropriate time, and progress was monitored by TLC. Upon completion, the reaction mixture was cooled to room temperature, and ethanol (10 mL) was added. The mixture was stirred for 30 minutes to obtain the crude solid product. The solid was collected by

filtration using Whatman filter paper, washed thoroughly with cold ethanol and hexane to remove traces of aldehyde, and recrystallized from ethanol if necessary.

[5a] dimethyl 4-(4-chlorophenyl)-2,6-dimethyl-1,4-dihydropyridine-3,5-dicarboxylate [38]

Colour: White, **m.p.**: 254–256˚C **% Yield**: 88 ^{1}H NMR (400 MHz, $CDCl_3$) δ 7.25–7.12 (m, 4H), 5.78 (d, J = 14.8 Hz, 1H), 5.05–4.92 (m, 1H), 3.73–3.57 (m, 6H), 2.42–2.29 (m, 6H).^{13}C NMR (101 MHz, $CDCl_3$) δ 167.82, 145.97, 144.28, 131.82, 129.07, 128.13, 103.66, 51.03, 38.96, 19.59. FTIR Neat: cm^{-1}: 3324, 2952, 1725, 1647, 1481, 1381, 1221, 1174, 1015, 857, 757.

[5b] dimethyl 2,6-dimethyl-4-(3-nitrophenyl)-1,4-dihydropyridine-3,5-dicarboxylate [54]

Colour: White, **m.p.**: 124–126, **% Yield**: 90, ^{1}H NMR (400 MHz, $CDCl_3$) δ 8.28–7.86 (m, 2H), 7.76–7.50 (m, 1H), 7.50–7.21 (m, 1H), 6.04 (s, 1H), 5.30–4.96 (m, 1H), 3.84–3.45 (m, 6H), 2.61–2.16 (m, 6H). ^{13}C NMR (101 MHz, $CDCl_3$) δ 167.58, 149.59, 148.38, 145.09, 134.21, 128.74, 122.73, 121.42, 103.08, 51.15, 39.64, 19.57. FTIR Neat: cm^{-1}: 3341, 2949, 1727, 1697, 1646, 1430, 1342, 1216, 1118, 1017, 836, 763.

[5c] dimethyl 2,6-dimethyl-4-phenyl-1,4-dihydropyridine-3,5-dicarboxylate [38]

Colour: White, **m.p.**: 258–260˚C **% Yield**: 87, ^{1}H NMR (400 MHz, $CDCl_3$) δ 7.44–6.95 (m, 6H), 5.83 (d, J = 46.3 Hz, 1H), 5.18–4.87 (m, 1H), 3.84–3.46 (m, 7H), 2.56–2.12 (m, 7H).^{13}C NMR (101 MHz, $CDCl_3$) δ 168.11, 147.44, 144.34, 128.17, 128.04, 127.62, 126.21, 103.83, 77.38, 77.06, 76.74, 51.00, 39.29, 19.52, 17.07. FTIR Neat: cm^{-1}: 3363, 2949, 1678, 1650, 1483, 1377, 1224, 1125, 1014, 841, 746.

[5d] dimethyl 4-(4-methoxyphenyl)-2,6-dimethyl-1,4-dihydropyridine-3,5-dicarboxylate[28]

Colour: White, **m.p.**: 258–260˚C **% Yield**: 85, ^{1}H NMR (400 MHz, $CDCl_3$) δ 7.25–7.14 (m, 2H), 6.87–6.65 (m, 2H), 5.95 (d, J = 13.4 Hz, 1H), 5.03–4.88 (m, 1H), 3.81–3.73 (m, 3H), 3.65 (d, J = 15.2 Hz, 6H), 2.40–2.25 (m, 6H). ^{13}C NMR (101 MHz, $CDCl_3$) δ 168.19, 157.96, 144.13, 140.00, 129.63, 128.60, 113.96, 113.41, 104.02, 55.34, 55.14, 50.99, 38.43, 19.50. FTIR Neat: cm^{-1}: 3347, 2952, 1702, 1643, 1482, 1377, 1215, 1124, 1015, 827, 744.

[5e] dimethyl 4-(4-hydroxyphenyl)-2,6-dimethyl-1,4-dihydropyridine-3,5-dicarboxylate[38]

Colour: White, **m.p.**: 300–302˚C **% Yield**: 86, ^{1}H NMR (400 MHz, $CDCl_3$) δ 7.83 (s, 1H), 7.34–7.19 (m, 1H), 7.05 (d, J = 8.5 Hz, 2H), 6.68 (t, J = 17.0 Hz, 2H), 4.87 (s, 1H), 3.76–3.42 (m, 6H), 2.29 (s, 6H). ^{13}C NMR (101 MHz, $CDCl_3$) δ 168.33, 155.12, 144.45, 139.12, 128.56, 115.61, 114.91, 103.73, 50.80, 40.46, 40.26, 40.05, 39.84, 39.63, 38.25, 19.23. FTIR Neat: cm^{-1}: 3353, 2954, 1730, 1683, 1646, 1482, 1378, 1213, 1097, 1023, 857, 752.

[5f] diethyl 4-(4-chlorophenyl)-2,6-dimethyl-1,4-dihydropyridine-3,5-dicarboxylate [30]

Colour: White, **m.p.**: 144–146˚C **% Yield**: 91, ^{1}H NMR (400 MHz, $CDCl_3$) δ 7.39–7.00 (m, 4H), 5.86 (d, J = 91.4 Hz, 1H), 5.14–4.72 (m, 1H), 4.39–3.86 (m, 4H), 2.46–2.23 (m, 6H), 1.43–1.04 (m, 6H). ^{13}C NMR (101 MHz, $CDCl_3$) δ 167.54, 146.38, 144.20, 131.70, 129.41, 127.95, 103.77, 59.84, 39.26, 19.50, 14.27. FTIR Neat: cm^{-1}: 3347, 2982, 1726, 1678, 1512, 1486, 1367, 1270, 1208, 1118, 1026, 858, 751, 692.

[5g] diethyl 4-(4-hydroxy-3-methoxyphenyl)-2,6-dimethyl-1,4-dihydropyridine-3,5-dicarboxylate

Colour: White, **m.p.**:188–190, **% Yield**: 88, ^{1}H NMR (400 MHz, $CDCl_3$) δ 6.98–6.67 (m, 6H), 5.82–5.33 (m, 4H), 5.09–4.83 (m, 2H), 4.29–3.93 (m, 8H), 3.96–3.71 (m, 6H), 2.48–2.19 (m, 11H), 1.34–1.14 (m, 11H). ^{3}C NMR (101 MHz, $CDCl_3$) δ 167.79, 145.75, 143.82, 143.57, 140.02, 120.49, 113.79, 110.83, 104.33, 59.72, 55.66, 39.15, 19.51, 14.51. FTIR Neat: cm^{-1}: 3354, 2987, 1693, 1647, 1483, 1370, 1296, 1209, 1115, 1014, 826, 743, 694.

[6a] methyl 4-(4-chlorophenyl)-2,7,7-trimethyl-5-oxo-1,4,5,6,7,8-hexahydroquinoline-3-carboxylate [16]

Colour: White, **m.p.**: 218–220˚C **% Yield**: 89, ^{1}H NMR (400 MHz, DMSO) δ 9.16 (s, 1H), 7.33–7.06 (m, 4H), 4.85 (s, 1H), 3.52 (s, 3H), 2.47–2.37 (m, 1H), 2.30 (s, 3H), 2.30–2.10 (m, 2H), 1.98 (d, J = 16.0 Hz, 1H), 1.00 (s, 3H), 0.82 (s, 3H). ^{13}C NMR (101 MHz, DMSO) δ 194.78, 167.62, 150.11, 146.88, 146.19, 130.71, 129.62, 128.27, 110.16, 103.24, 51.19, 50.63, 39.79, 35.85, 32.61, 29.55, 26.87, 18.79. FTIR Neat: cm^{-1}: 3195, 2955, 1741, 1679, 1486, 1381, 1223, 1111, 1004, 885, 775.

[6b] methyl 4-(4-hydroxy-3-methoxyphenyl)-2,7,7-trimethyl-5-oxo-1,4,5,6,7,8-hexahydroquinoline-3-carboxylate

Colour: White, **m.p.**: 274–276, **% Yield**: 88, ^{1}H NMR (400 MHz, DMSO) δ 8.81 (d, J = 171.0 Hz, 2H), 6.84–6.24 (m, 3H), 4.78 (s, 1H), 3.62 (d, J = 45.3 Hz, 6H), 2.42 (d, J = 17.0 Hz, 1H), 2.29 (d, J = 12.1 Hz, 4H), 2.18 (d, J = 16.1 Hz, 1H), 2.00 (d, J = 16.1 Hz, 1H), 0.95 (d, J = 52.7 Hz, 6H). ^{13}C NMR (101 MHz, DMSO) δ 194.84, 167.99, 149.72, 147.37, 145.13, 145.10, 139.35, 119.86, 115.49, 112.45, 112.32, 110.73, 104.21, 56.03, 55.95, 51.02, 50.83, 39.87, 35.33, 32.58, 29.69, 26.90, 18.70. FTIR Neat: cm^{-1}: 3187, 2945, 1741, 1695, 1484, 1378, 1215, 1104, 1028, 857, 165.

[6c] methyl 2,7,7-trimethyl-5-oxo-4-phenyl-1,4,5,6,7,8-hexahydroquinoline-3-carboxylate [17]

Colour: White, **m.p.**: 210–212˚C **% Yield**: 87, ^{1}H NMR (400 MHz, DMSO) δ 9.07 (d, J = 19.9 Hz, 1H), 7.24–6.99 (m, 5H), 4.88 (s, 1H), 3.53 (s, 3H), 2.42 (d, J = 17.1 Hz, 1H), 2.35–2.24 (m, 4H), 2.16 (t, J = 13.2 Hz, 1H), 1.99 (d, J = 16.0 Hz, 1H), 1.05–0.96 (m, 3H), 0.84 (s, 3H). ^{13}C NMR (101 MHz, DMSO) δ 194.88, 167.85, 150.07, 147.94, 145.76, 128.30, 127.73, 126.19, 110.48, 103.76, 51.12, 50.71, 39.72, 36.11, 32.59,

29.59, 26.88, 18.74. FTIR Neat: cm^{-1}: 3200, 3076, 2944, 1738, 1705, 1604, 1483, 1377, 1211, 1106, 1023, 885, 761.

[6d] methyl 2,7,7-trimethyl-4-(3-nitrophenyl)-5-oxo-1,4,5,6,7,8-hexahydroquinoline-3-carboxylate [49]

Colour: White, **m.p.**: 218–220, **% Yield**: 90, ^{1}H NMR (400 MHz, DMSO) δ 9.29 (s, 1H), 8.07–7.81 (m, 2H), 7.56 (dt, J = 28.3, 7.8 Hz, 2H), 4.99 (s, 1H), 3.53 (s, 3H), 2.46 (d, J = 17.1 Hz, 1H), 2.37–2.27 (m, 4H), 2.19 (t, J = 12.0 Hz, 1H), 1.99 (d, J = 16.2 Hz, 1H), 1.07–0.96 (m, 3H), 0.80 (d, J = 19.5 Hz, 3H). ^{13}C NMR (101 MHz, DMSO) δ 194.88, 167.43, 150.66, 149.98, 148.01, 146.81, 134.61, 129.93, 122.18, 121.43, 109.70, 102.81, 51.30, 50.49, 39.75, 36.63, 32.65, 29.52, 26.74, 18.85. FTIR Neat: cm^{-1}: 3210, 3079, 2942,1739, 1697, 1617, 1480, 1378, 1285, 1104, 1006, 824, 776.

[6e] ethyl 4-(4-fluorophenyl)-2,7,7-trimethyl-5-oxo-1,4,5,6,7,8-hexahydroquinoline-3-carboxylate [56]

Colour: White, **m.p.**: 180–182˚C **% Yield**: 90, ^{1}H NMR (400 MHz, DMSO) δ 9.12 (s, 1H), 7.16 (dd, J = 8.7, 5.7 Hz, 2H), 6.99 (t, J = 8.9 Hz, 2H), 4.84 (s, 1H), 4.05–3.90 (m, 2H), 2.41 (d, J = 17.0 Hz, 1H), 2.29 (d, J = 9.4 Hz, 4H), 2.17 (d, J = 16.2 Hz, 1H), 1.97 (d, J = 16.1 Hz, 1H), 1.11 (t, J = 7.1 Hz, 3H), 1.00 (s, 3H), 0.82 (s, 3H). ^{13}C NMR (101 MHz, DMSO) δ 195.06, 167.29, 162.09, 159.69, 150.21, 145.64, 144.29, 144.26, 129.64, 129.56, 114.91, 114.70, 110.35, 104.02, 59.62, 50.61, 39.78, 35.76, 32.56, 29.51, 26.84, 18.68, 14.55. FTIR Neat: cm^{-1}: 3284, 3081, 2957, 1797, 1695, 1480, 1379, 1276, 1104, 1027, 877, 758.

[6f] ethyl 2,7,7-trimethyl-5-oxo-4-(p-tolyl)-1,4,5,6,7,8-hexahydroquinoline-3-carboxylate [44]

Colour: White, **m.p.**: 256–258˚C **% Yield**: 89, ^{1}H NMR (400 MHz, DMSO) δ 9.02 (s, 1H), 7.03 (d, J = 8.1 Hz, 2H), 6.98 (d, J = 8.0 Hz, 2H), 4.81 (s, 1H), 3.97 (q, J = 7.1 Hz, 2H), 2.41 (d, J = 17.0 Hz, 1H), 2.32–2.25 (m, 4H), 2.22–2.12 (m, 4H), 1.97 (d, J = 16.0 Hz, 1H), 1.14 (t, J = 7.1 Hz, 3H), 1.01 (s, 3H), 0.85 (s, 3H). ^{13}C NMR (101 MHz, DMSO) δ 194.77, 167.38, 149.89, 145.23, 145.16, 135.01, 128.75, 127.81, 110.55, 104.30, 59.48, 50.74, 39.75, 35.86, 32.58, 29.61, 26.94, 21.02. FTIR Neat: cm^{-1}: 3190, 3078, 2956, 1803, 1697, 1488, 1384, 1279, 1105, 1028, 848, 737.

[6g] ethyl 4-(4-methoxyphenyl)-2,7,7-trimethyl-5-oxo-1,4,5,6,7,8-hexahydroquinoline-3-carboxylate [57]

Colour: White, **m.p.**: 258–260˚C **% Yield**: 86, ^{1}H NMR (400 MHz, DMSO) δ 9.00 (s, 1H), 7.06 (d, J = 8.7 Hz, 2H), 6.74 (d, J = 11.6 Hz, 2H), 4.80 (s, 1H), 3.98 (q, J = 7.1 Hz, 2H), 3.67 (s, 3H), 2.41 (d, J = 17.0 Hz, 1H), 2.34–2.25 (m, 4H), 2.16 (d, J = 16.1 Hz, 1H), 1.98 (d, J = 16.0 Hz, 1H), 1.14 (t, J = 7.1 Hz, 3H), 1.01 (s, 3H), 0.86 (s, 3H). ^{13}C NMR (101 MHz, DMSO) δ 194.74, 167.41, 157.76, 149.70, 145.07, 140.49, 128.86, 113.56, 110.68, 104.41, 59.45, 55.33, 50.77, 39.81, 35.39, 32.59, 29.61, 26.99, 18.72, 14.64. FTIR Neat: cm^{-1}: 3199, 3074, 2956, 1802, 1698, 1491, 1379, 1276, 1105, 1031, 847, 765.

Result and discussion

A Brønsted amino acid ionic liquid (AAIL), proline methane sulphonate (ProMSA) [60], was employed as a catalyst for the synthesis of a series of dihydropyridine derivatives (**5a-5g and 6a-6g**). The reaction conditions were systematically optimized by evaluating key parameters, including temperature, solvent effects, and catalyst loading. To establish the optimal conditions, the synthesis of dimethyl 4-(4-chlorophenyl)-2,6-dimethyl-1,4-dihydropyridine-3,5-dicarboxylate (**5a**) was selected as a model reaction. This compound was prepared via a multicomponent reaction of 4-chlorobenzaldehyde (**1**), methyl acetoacetate (**2**), and ammonium acetate (**3**) (Scheme 1). The reaction was investigated using various catalyst concentrations and at different temperatures; the results of this optimization study are summarized in Table 1. In preliminary experiments, the model reaction was heated at 60°C for 3 hours in the absence of a catalyst; no product formation was observed by TLC (Table 1, **entry 1**). Subsequently, the reaction was investigated using 5 mol% catalysts at 80˚C. As the reaction time was extended from one to three hours, the product yield increased marginally from 30% to 46% (Table 1, **entries 2–4**). Increasing the catalyst loading to 10 mol% and raising the temperature to 100˚C further improved the yield from 36% to 55% (Table 1, **entries 5 and 6**). The optimal result was achieved under solvent-free conditions using 10 mol% catalyst at 100˚C for one hour, affording the desired product in 91% yield (Table 1, **entry 7**). It is noteworthy that no significant increase in yield was observed when the temperature was raised above 100˚C or when the catalyst loading was increased from 10 to 20 mol% (Table 1, **entries 8–10**). Additionally, the reaction was performed in various solvents, including ethanol, water, and a water-ethanol mixture. The results indicate that solvent choice significantly influences reaction efficiency, with all tested solvents affording relatively low yields compared to solvent-free conditions (Table 1, **entries 11–13**).

Table 1
Optimization of reaction conditions for the synthesis of **5a**

Entry	ProMSA (mol %)	Solvent	Temperature (^{0}C)	Time (h)	% Yield [b]
1	-	-	**60**	**3**	-
2	5	-	80	1	30
3	5	-	80	2	39
4	5	-	80	3	46
5	10	-	80	1	36
6	10	-	80	3	55
7	**10**	**-**	**100**	**1**	**91**
8	10	-	100	2	90
9	20	-	100	1	89
10	10	-	120	1	87
11	10	Ethanol	Reflux	2	71
12	10	Water	Reflux	2	-
13	10	Water-Ethanol	Reflux	2	42

[a] Reaction condition: 4-chlorobenzaldehyde (**10 mmol**), methyl acetoacetate (**20 mmol**), ammonium acetate (**20 mmol**) and catalyst ProMSA, [b] Isolated yield, [c] Optimized condition shown in bold

A series of dihydropyridine derivatives were synthesized via a multicomponent condensation reaction catalyzed by **ProMSA** under solvent-free conditions (Scheme 2). The reaction afforded the desired products in excellent yields, ranging from 86% to 91%, as summarized in Table 2. Due to the good solubility of the **ProMSA** catalyst in ethanol, it could be readily separated from the reaction mixture. To explore the substrate scope, a variety of aromatic aldehydes bearing both electron-donating groups (e.g., -CH_3, -OH, -OCH_3) and electron-withdrawing groups (e.g., halides, -NO_2) were employed. Aldehydes containing electron-withdrawing substituents reacted more rapidly and afforded slightly higher product yields compared to those with electron-donating groups. A total of fourteen dihydropyridine derivatives (**5a-5g and 6a-6g**, Table 2) were successfully synthesized in moderate to excellent yields. All synthesized compounds were characterized by their physical properties, such as melting point, and spectroscopic techniques, including FTIR, ^{1}H NMR, and ^{13}C NMR spectroscopy. The synthesis of 1,4-dihydropyridine derivatives was investigated via a three-component reaction involving aromatic aldehydes, β-keto esters, and ammonium acetate, catalyzed by **ProMSA**, a Brønsted amino acid ionic liquid (AAIL). Under optimized conditions, all substrates reacted smoothly with 10 mol% of the AAIL under solvent-free conditions,

affording the desired 1,4-dihydropyridine derivatives (**5a-5g and 6a-6g**, Table 2) in moderate to excellent yields. Both electron-rich and electron-deficient aldehydes performed well, giving comparable product yields.

Table 2 One-pot synthesis of 1, 4-dihyropyridine derivatives (**5a-5g** and **6a-6g**)

Entry	R_1	β-keto esters	% Yield[c]	Melting Point ^0C	
				Observed[d]	Reported
5a	4-Cl	MAA/MAA	91	254–256	257–258
5b	3-NO_2	MAA/MAA	90	124–126	125–127
5c	H	MAA/MAA	87	258–260	259–261
5d	4-OCH_3	MAA/MAA	85	258–260	257–259
5e	4-OH	MAA/MAA	86	300–302	297–298
5f	4-Cl	EAA/EAA	91	144–146	145–146
5g	3-OCH_3,4-OH	EAA/EAA	88	188–190	-
6a	4-Cl	MAA/DM	89	218–220	221–223
6b	3-OCH_3,4-OH	MAA/DM	88	236–238	-
6c	H	MAA/DM	87	210–212	212–214
6d	3-NO_2	MAA/DM	90	218–220	221–223
6e	4-F	EAA/DM	90	180–182	180–182
6f	4-CH_3	EAA/DM	89	256–258	258–260
6g	4-OCH_3	EAA/DM	86	258–260	258–259

[a]All aldehydes available commercially and were used as received. MAA: methyl acetoacetate, EAA; Ethyl acetoacetate, DM: Dimedone, [b]The progress of reaction was followed by TLC, [c]Refers to yield of isolated products. [d]All the products have been reported previously and characterized by comparison of their points with the literature values.

As a representative example, the structure of dimethyl 4-(4-chlorophenyl)-2,6-dimethyl-1,4-dihydropyridine-3,5-dicarboxylate (**5a**) was unequivocally established by spectroscopic analysis. The ^1H NMR spectrum of **5a** exhibited a multiplet at δ 7.25–7.12 integrating for four protons, corresponding to the aromatic protons (C-18, C-19, C-21, and C-22). A doublet at δ 5.78 integrating for one proton was assigned to the amine proton (N-3). A multiplet at δ 5.05–4.92 integrating for one proton was attributed to the methylene proton at C-6. Multiplets at δ 3.73–3.57 integrating for six protons corresponded to the

methoxy groups of the esters (C-12 and C-17). Another multiplet at δ 2.40–2.29 integrating for six protons was assigned to the methyl groups at C-7 and C-8. The ^{13}C NMR spectrum displayed three aliphatic carbon signals: a methylene at δ 19.59 (C-6), methyl carbons at δ 38.96 (C-7 and C-8), and methoxy carbons at δ 51.03 (C-17 and C-18). The eight aromatic carbons resonated in the region δ 103.66–145.97 (C-1, C-2, C-4, C-5, C-13, and C-18 to C-22), while the ester carbonyl carbon appeared at δ 167.82, confirming the structure of compound **5a**. The FTIR spectrum further supported the structure, showing characteristic absorption bands at 3324 cm^{-1} (N–H stretching), 2952 cm^{-1} (C–H stretching), and 1725 cm^{-1} (ester carbonyl stretching).

The catalytic activity of **ProMSA** was compared with previously reported catalysts for the synthesis of dihydropyridine derivatives, considering key parameters such as reaction time, temperature, solvent, and isolated product yield. **ProMSA** demonstrated superior performance, affording moderate to excellent yields under solvent-free conditions with a short reaction time of just 60 minutes (Table 2, **entry 12**). In contrast, several literature catalysts required organic solvents and longer reaction times ranging from 8 to 300 minutes to achieve comparable yields, often at different temperatures.

Table 3
Comparison of the activity of different catalysts with **ProMSA**

Entry	Name of the catalyst	Time (min)	T (˚C)	% Yield
1	Alumina sulphuric acid (ASA)	120–300	70	82–95 [11]
2	Polyphosphoric acid (PPA)@NiO	40	40	94–97 [21]
3	Tetrabutylammonium hydrogen sulfate	55–90	70	65–80 [25]
4	Sulfonic acid functionalized pyridinium chloride	8–12	50	76–96 [28]
5	Manganese ferrite nanoparticles ($MnFe_2O_4$)	14–90	RT	80–94 [31]
6	Nano-MgO–ZrO_2 metal oxide	15	RT	95 [34]
7	Hercynite@sulfuric acid	15–115	100	80–97 [37]
8	Silica-Coated $NiFe_2O_4$ nanoparticles	10–60	120	65–94 [40]
9	Bismuth (III) chloride	15–20	70	83–96[46]
10	Aluminized polyborate	10–30	100	85 [48]
11	MCM-41 supported cobalt (II) complex	10	130	90 [50]
12	**ProMSA**	**60**	**100**	**86–91 Present Work**

Mechanism of reaction:

A plausible mechanism for the formation of 1,4-dihydropyridine derivatives catalyzed by **ProMSA** is proposed in **Scheme 3**. Initially, the Brønsted acidic ionic liquid **ProMSA** facilitates the conversion of the β-keto ester to its enol form, which subsequently reacts with the activated aldehyde to generate intermediate **A**. Concurrently; ammonium acetate generates ammonia, which reacts with another molecule of activated β-keto ester to form enamine **B**. The nucleophilic addition of enamine **B** to intermediate **A** affords intermediate **C**, which undergoes tautomerization to yield intermediate **D**. This intermediate then undergoes intramolecular nucleophilic attack by the NH_2 group on the activated carbonyl group, accompanied by the loss of a water molecule, to form intermediate **E**. Finally, tautomerization of **E** furnishes the desired 1,4-dihydropyridine derivative. Throughout the catalytic cycle, **ProMSA** plays a crucial role in activating the carbonyl groups via proton donation, with the proton being subsequently transferred back to the catalyst to regenerate it for subsequent cycles. This proposed mechanism is consistent with previously reported literature [28].

In-silico ADME analysis:

The ADME (Absorption, Distribution, Metabolism, and Excretion) profiles of potential drug candidates can be reliably predicted using computational tools, thereby increasing confidence in their suitability for further drug development. In this study, the SwissADME online server (http://swissadme.ch/) [61] was employed to evaluate the pharmacokinetic properties and drug-likeness of the synthesized compounds. This program reduces the time and cost associated with early-stage research by rapidly assessing oral bioavailability and drug-relevant features based on established filters, including Lipinski's rule of five.

Table 4
ADME study of docked dihydropyridine derivatives

Entry	MW	H-bond acceptors	H-bond donors	iLOGP	Rotatable bonds	TPSA	WLOGP	MR	Heavy atoms
1	335.78	4	1	3.24	5	64.63	2.54	90.71	23
2	346.33	6	1	2.68	6	110.5	1.79	94.52	25
3	346.33	6	1	2.68	6	110.5	1.79	94.52	25
4	331.36	5	1	3.29	6	73.86	1.9	92.19	24
5	317.34	5	2	2.68	5	84.86	1.59	87.73	23
6	359.85	3	1	3.39	3	55.4	3.74	101.67	25
7	371.43	5	2	3.23	4	84.86	2.8	105.18	27
8	325.4	3	1	3.1	3	55.4	3.08	96.66	24
9	370.4	5	1	2.9	4	101.2	2.99	105.49	27
10	363.84	4	1	3.59	7	64.63	3.32	100.33	25
11	375.42	6	2	3.37	8	94.09	2.38	103.83	27
12	357.42	4	1	3.48	4	55.4	4.03	101.43	26
13	353.45	3	1	3.57	4	55.4	3.78	106.44	26
14	369.45	4	1	3.49	5	64.63	3.48	107.96	27

The ADME prediction tool evaluates a range of key physicochemical and pharmacokinetic parameters, such as molecular weight (MW), gastrointestinal absorption (HIA), blood-brain barrier permeability (BBB), P-glycoprotein substrate status (Pgp), number of hydrogen bond donors (nHBD) and acceptors (nHBA), bioavailability score (BS), topological polar surface area (TPSA), lipophilicity (WLOGP), drug-likeness (DL), and drug score (DS). The predicted ADME data for all synthesized compounds are presented in Table 4. The boiled-Egg model provides a predictive assessment of passive gastrointestinal absorption (HIA) and blood-brain barrier (BBB) penetration [62]. As illustrated in Fig. 2, the results indicate that compounds **2, 3, 4, 5, 7, 9, and 11** are located in the white region (outside the yolk), predicting high gastrointestinal absorption but no BBB permeation.

In contrast, derivatives **1, 6, 8, 10, 12, 13, and 14** were positioned in the yolk (BBB-permeable region), suggesting they can passively cross the blood-brain barrier and are not effluxed by P-glycoprotein, thereby enabling these molecules to reach therapeutically relevant concentrations within the brain. The physicochemical parameters related to drug-likeness, based on Lipinski's rule of five, are summarized in Table 4 and illustrated graphically in Fig. 2. Lipophilicity [63] was evaluated using multiple computational models, including iLOGP, XLOGP3, WLOGP, MLOGP, and Silicos-IT, with consensus LOGP values ranging

from approximately 1.59 to 4.03. This range reflects moderate lipophilicity, which is generally favorable for oral drug candidates. The predicted aqueous solubility (ESOL Log S) values ranged from approximately − 3.1 to − 4.5, indicating a moderate to low solubility characteristic that falls within an acceptable range for oral bioavailability. Compounds with higher Log P values exhibited lower solubility, which is associated with enhanced membrane permeability and an increased likelihood of crossing the blood-brain barrier. In contrast, less lipophilic analogues are predicted to favor peripheral distribution. Overall, the *in silico* ADME results confirm that all synthesized compounds satisfy the established drug-likeness criteria. Lipinski's rule such as (MW: ≤ 500; logP: ≤ 4–15; H-bond acceptor ≤ 10; H-bond donor ≤ 5; Molar refractivity (*MR*) is in between 40–130), Veber rule (TPSA ≤ 140 A˚; rotatable bonds ≤ 10), Ghose filter (MW: ≤ 500; logP: ≤ 4–15; MR: 40–130), Egan rule (logP: ≤ 4–15; TPSA ≤ 140 A˚), and Muegge (MW: ≤ 500; logP: ≤ 4–15; H-bond acceptor ≤ 10; H-bond donor ≤ 5;) not violate the guidelines indicating favorable physicochemical properties, good oral absorption potential, and suitability for further pharmacokinetic evaluation. In the present series, compounds exhibiting low topological polar surface area (TPSA) combined with moderate to high lipophilicity (LOGP) were consistently predicted to be blood-brain barrier (BBB) permeable. The most favorable predictions for central nervous system (CNS) indications were observed for entries **1, 6, 8, 10, 12, 13, and 14**, which collectively demonstrate an optimal balance of negligible P-glycoprotein substrate liability, BBB permeability, and high gastrointestinal absorption. Among these, compounds **6, 12, and 13** possess the lowest TPSA values, a characteristic that enhances CNS exposure but is also associated with reduced aqueous solubility and a potentially higher risk of metabolic interactions. Notably, the absence of CYP2D6 inhibition across the entire series significantly reduces the likelihood of serious CNS-related drug-drug interactions. Overall, compounds **6, 8, 12, and 13** emerge as the most promising CNS-focused leads, achieving a favorable balance between BBB penetration, oral absorption, and manageable metabolic risk.

Conclusion

In conclusion, we have developed an efficient protocol for the one-pot, multicomponent synthesis of 1,4-dihydropyridine derivatives. The reaction employs aromatic aldehydes, β-keto esters, and ammonium acetate in the presence of a catalytic amount of a Brønsted acidic amino acid ionic liquid (**ProMSA**) under solvent-free conditions. The advantages of this methodology include the use of a readily available and inexpensive catalyst, mild reaction conditions, a simple work-up procedure, and the attainment of moderate to excellent product yields without the need for special precautions. This developed protocol represents a simple, environmentally benign, and safer synthetic approach. Furthermore, all synthesized compounds satisfied the Lipinski, Veber, Ghose, Egan, and Muegge drug-likeness criteria, indicating favorable physicochemical properties, good oral absorption potential, and suitability for further pharmacokinetic evaluation.

Declarations

Conflict of Interest

Authors declares no conflict of interest.

Author Contribution

Author Nitin Rode developed the methodolgy for the synthesis of dihydropyridines and wrote the result and discussion section of the manuscript.Author Kishor Kale wrote the introduction and ADME profoling of the synthesised compunds.Author Santosh Terdale and other authors reviewed the manuscript.

Supplementary Information The online version contains supplementary material available at http://doi.org/10.1007/s11164-026-xxxxx-x.

References

1. A. Hantzsch Justus L. Ann. Cheime. **215**, 1 (1882).
2. S. S. Makone, S. N. Niwadange, Der Chemica Sinica, **3(5)**, 1293 (2012).
3. M. F. Litvic, M. Litvic , I. Cepanec, V. Vinkovic. Molecule, **12**, 2546 (2007).
4. M. M. Heravi, V. Zadsirjan, RSC Adv., 10 44247 (2020).
5. E. Frank, G. Szollosi, Molecule, **26**, 4617 (2021).
6. M. C. Sanu, J. Joseph, D. Chacko, Int. J. Pharm. Sci. Rev. Res., **69(2)**, 64 (2021).
7. S. Bijani, D. Iqbal, S. Mirza, V. Jain, S. Jahan, M. Alsaweed, Y. Madkhali, S. A. Alsagaby, S. Banawas, A. Algarni, F. Alrumaihi, R. M. Rawal, W. Alturaiki, A. Shah, Life, **12**, 519 (2022).
8. A. Mermer, T. Keles, Y. Sirin, Bioorg. Chem., **114**, 1 (2021).
9. S. Indumathi, R. Karthikeyan, A. J. A. Nasser, A. Idhayadhulla, R. S. Kumar, J. Chem. Pharm. Res.,**7(2)**, 434 (2015).
10. A. R. Ninan, R. Babbar, S. Dhiman , T. G. Singh, K. Kaur, V. Dhiwan, Biointerface research in applied chemistry, **12(3)**, 3117 (2022).
11. G. Swarnalatha, G. Prasanthi, N. Sirisha, C. M. Chetty, International Journal of ChemTech Research, **3(1)**, 75 (2011).
12. R. S. Thombal, V. H. Jadhav, Chemistry & Applied Biochemistry, **2(1)**, 1 (2015)
13. M. Nikpassand, M. Mamaghani, K. Tabatabaeian, Molecules, **14**, 1468 (2009).
14. M. G. Sharma, D. P. Rajani, H. M. Patel, R. Soc. open sci., **4**, 1 (2017).
15. Y. Liu, J. Liu, X. Wang, T. Cheng, R. Li, Tetrahedron, **69**, 5242 (2013).
16. R. Surasani, D. Kalita, A. V. D. Rao, K. Yarbagi, K. B. Chandrasekhar, **135**, 91(2012).
17. M. Reza, P. Heravi, S. Mehranfar and N. Shabani, Comptes rendus - Chimie, 1(2013).
18. W. A. Silva, S. Cristina, S. Takada, C. C. Gatto, I. V. Maravalho, Catalyst, **16(96)**, 1 (2026).
19. S. Ghoderao, P. Bandivadekar, G. U. Chaturbhuj, Results in Chem., **7**, 101407(2024).
20. S. Patil, P.B. Pawar, S.D. Jadhav, M.B. Deshmukh , Asian Journal of Chemistry, **25(17)**, 9442 (2013).

21. K. S. Patil, S. T. Mane, S. S. Mohite, D. G. Kanase, J. Nanoparticle Res., **26**, 1 (2024).
22. T. Momeni, M. M. Heravi, T. Hosseinnejad , M. Mirzaei, J. Mol. Struct., **1199**, 127011 (2020).
23. M. Yosefzadeh, M. Mokhtary, Iranian Journal of Catalysi, **6(2)**, 153 (2016).
24. S. Askari, M. Mehdi, M. Jafarzadeh, Catal. Letters, **152**, 1517 (2022).
25. V. Goel, A. Bajwan, S. Chauhan, S. Goel, Chem. Sci. Trans., **7(2)**, 343 (2018).
26. H. R. Memarian, I. Mohammadpoor-baltork, M. Javahery, Journal of the Chinese Chemical Society, **53**, 511 (2006).
27. M. Ghorbani, H. Reza, S. Noura, F. Khammar, K. Behbodi, B. Reisi, M. Oftadeh, J. Mol. Liq., **204**, 15 (2015).
28. A. Khazaei, M. Ali, A. Reza, M. Zare, J. Afsar, A. Zare, V. Khakyzadeh, M. H. Beyzavi, Chinese J. Catal., **34**, 1936 (2013).
29. R. P. Kagne, G. Nikam, V. G. Kalalawe, S. N. Niwadange, D R. Munde, Journal of Chemistry and Chemical Sciences, **7(11)**, 1064 (2017).
30. A. Teimouri1, L. Ghorbanian, A. Moatari, Bull. Chem. Soc. Ethiop., **27(3)**, 427 (2013).
31. N. Ahadi, A. Mobinikhaledi, M. A. Bodaghifard, Appl. Organomet. Chem., 18 (2020).
32. Z. Abbas-ordoo, A. Mobinikhaledi, M. A. Bodaghifard , Heliyon, **10**, e37151(2024).
33. H. K. Askarani, M. A. K. Zarchi, B. F. Mirjalili, A. Bamoniri, Journal of the Iranian Chemical Society, **19**, 3189 (2022).
34. M. B. Gawande, A. K. Rathi, P. S. Branco, T. M. Potewar, A. Velhinho, I. D. Nogueira, A. Tolstogouzov, C. Amjad, A. Ghumman, Orlando M. N. D. RSC Adv., **3**, 3611 (2013).
35. K. Khosravi, A. Azizi, M. A. Zolfigol, F. Afsharnadery, Z. Nazari, Iranian Journal of Catalysis, **15**, 18 (2025).
36. H Cahyana, B Ardiansah, N S Aisyah, Materials Science and Engineering, **763**, 012035 (2020)
37. M. Mohammadi, A. Ghorbani-choghamarani, RSC Adv. **12**, 2770 (2022).
38. M.Yarie, M.A. Zolfigol, Y. Bayat,, A. Asgari, D. A. Alonso, A. Khoshnood, RSC Adv., 1(2013).
39. R. Zargartalebi, Z. Rafiee, Journal of Porous Material, (2025).
40. B. Maleki, A. V. Mofrad, R. Tayebee, A. Khojastehnezhad, H. Alinezhad, E. Rezaei Seresht, Russian Journal of General Chemistry, **87(12)**, 2922 (2017).
41. S. Moradi, M. Moradian, H. Naeimi, Acta Chim. Slov. **69**, 349 (2022).
42. P. Wu, L. Feng, Y. Liang, X. Zhang, B. Mahmoudi, M. Kazemnejadi, Applied Catal. A, Gen., 117301(2019).
43. R. M. Borade, S. B. Kale, P. P. Khirade, K. M. J. Rajendra, J. Inorg. Organomet. Polym. Mater., **34**, 1104 (2024).
44. A. Maleki, M. Kamalzare, M. Aghaei, J Nanostruct Chem, **5**, 95 (2015).
45. S. Das Sharma, P. Hazarika, D. Konwar, Catalysis Communications, **9**, 709 (2008).

46. C. V. N. Rao, S. Ramprasad, P. V. Rao, S. Subhani, Y. Gopi, Journal of Chemical and Pharmaceutical Research, **4(4)**, 2112 (2012).
47. T. Demirci, B. Çelik, Y. Yıldız, S. Eriş, M. Arslan, F. Sen, B. Kilbas, RSC Adv., **1** (2013).
48. D. Aute, A. Kshirsagar, B. Uphade, A. Gadhave, Research on Chemical Intermediates, **46**, 3491(2020).
49. F. Lashkari, R. Badri, E. Tahanpesar, React. Kinet. Mech. Catal., **134**, 361 (2021).
50. S. Sharma, U. P. Singh, A. P. Singh, Polyhedron, **199**, 115102 (2021).
51. B. B. F. Mirjalili, A. Bamoniri, L. A.Salmanpoor, J Nanostruct, **8(3)**, 276 (2018).
52. S. Aryanejad, G. Bagherzade, M. Moudi, New Journal of Chemistry, 1 (2020).
53. J. Yang, C. Jiang, J. Yang, C. Qian, D. Fang , Green Chemistry Letters and Reviews, **6(3)**, 262 (2013).
54. M. Nasr-esfahani, B. Karami, M. Behzadi, J. Heterocyclic Chem., **46**, 931 (2009).
55. B. Vijayakumar, Indian Journal of Advances in Chemical Science **1(2)**, 77 (2013).
56. D. Khan, N. Maurya, Russian Journal of Organic Chemistry, **59(4)**, 695 (2023).
57. B. S. Hote, T. A. J. Siddiqui, P. M. Pisal, Polycycl. Aromat. Compd., 1(2021).
58. K. Hussain, D. Wadhwa, International Journal of Organic Chemistry, **4**, 174 (2014).
59. K. Valadi, S. Gharibi, R. Taheri-ledari, A. Maleki, Solid State Sci., **101**, 106141 (2020).
60. N. R. Rode, A. A. Tantray, A. V Shelar, K. Pai, R. H. Patil, S. S. Terdale, Res. Chem. Intermed. **4**, (2023).
61. A. Daina, O. Michielin, V. Zoete, Sci. Rep. **7**, 42717 (2017).
62. A. Daina, V. Zoete, ChemMedChem , **11**, 1117 (2016).
63. A. Daina, O. Michielin, V. Zoete, J. Chem. Inf. Model, **51(12)**, 3284 (2014).

Figures

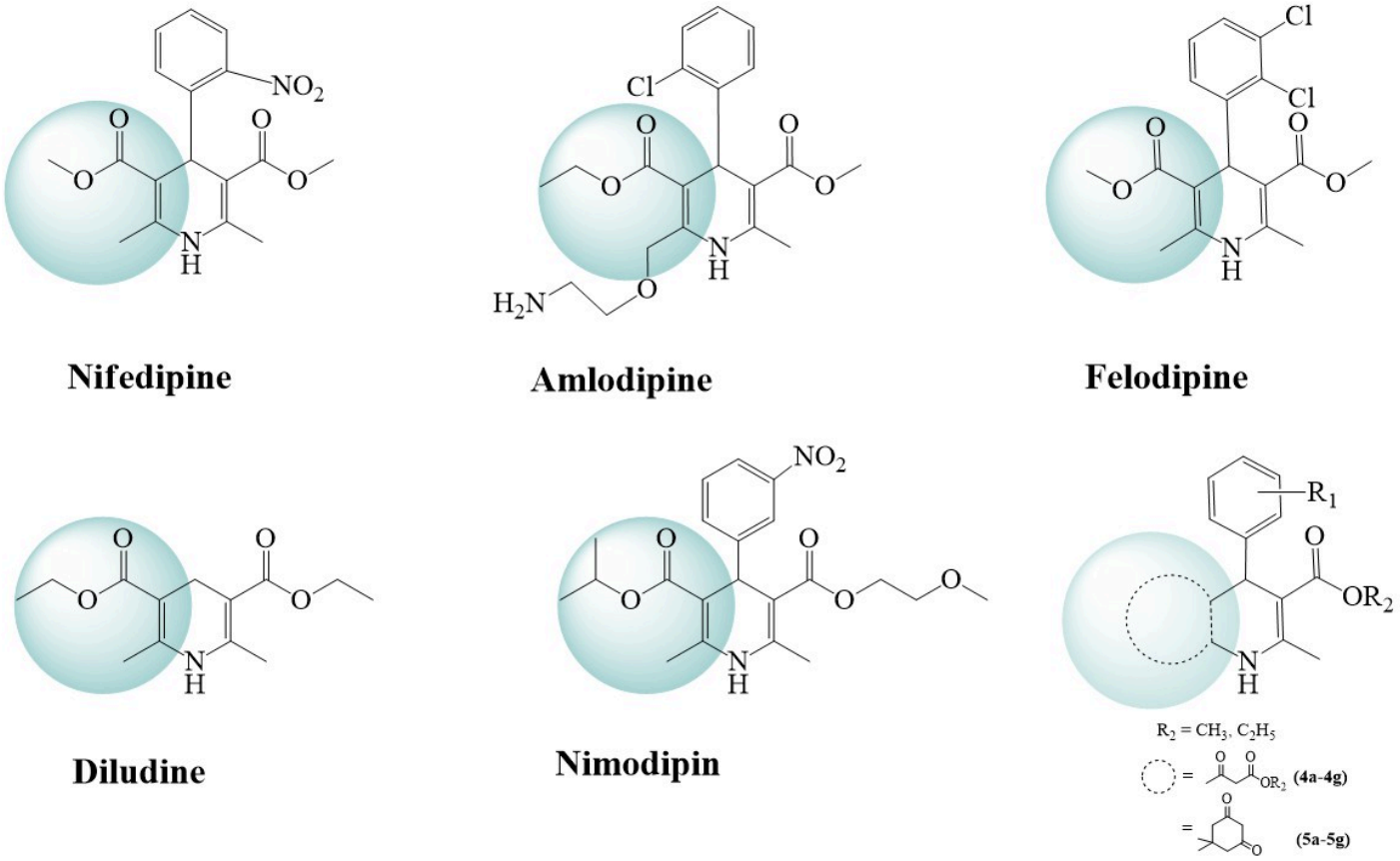


Figure 1

Biologically active dihydropyridine derivatives [12]

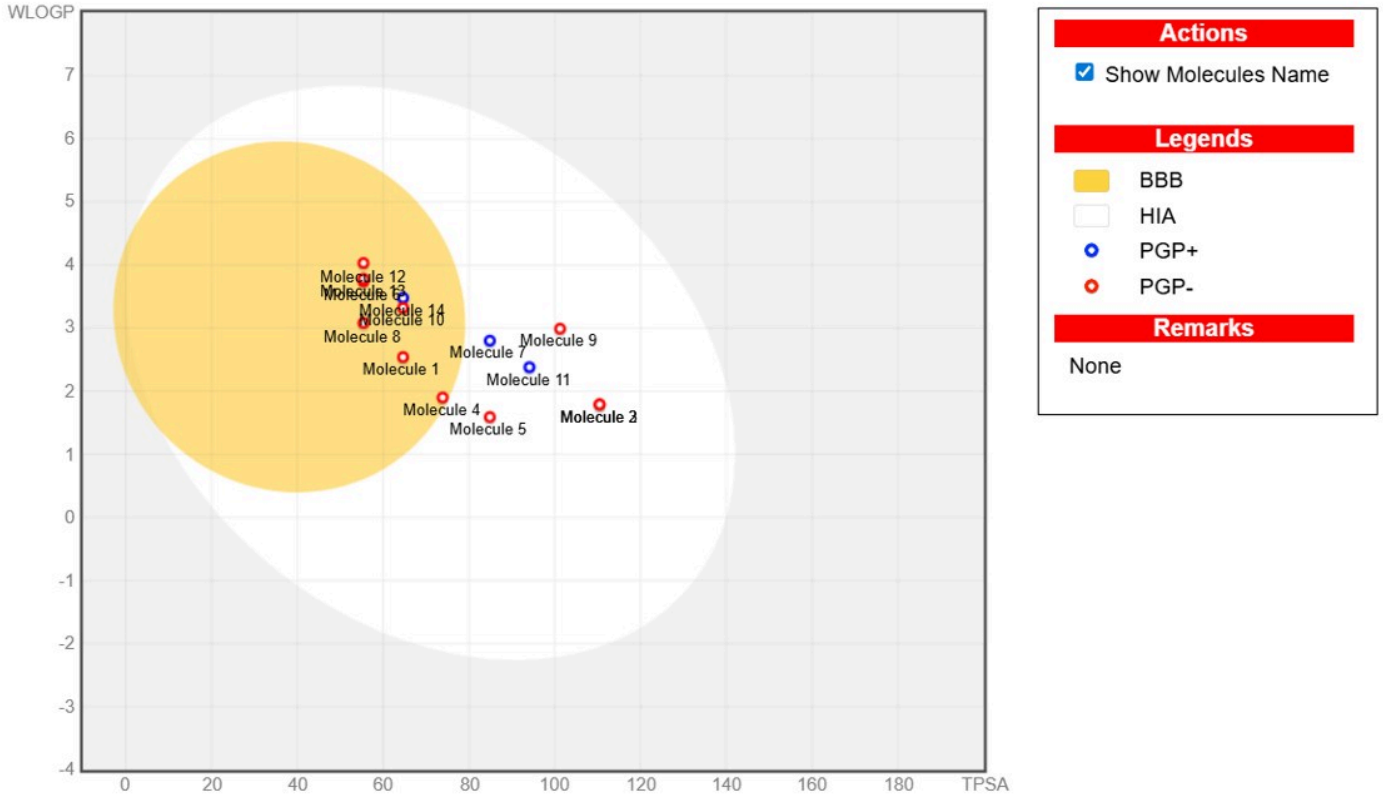


Figure 2

The BOILED-Egg as Function of the molecule in the WLogP versus TPSA for evaluation of passive HIA and BBB.

Supplementary Files

This is a list of supplementary files associated with this preprint. Click to download.

- SupplementaryMaterial.docx
- schem1.jpg
- schem2.jpg
- schem3.jpg